

# Laser induced formation of CsI ion clusters analyzed by delayed extraction time-of-flight mass spectrometry†

V. M. Collado,<sup>a</sup> F. A. Fernandez-Lima,<sup>ab</sup> C. R. Ponciano,<sup>a</sup> Marco Antonio Chaer Nascimento,<sup>c</sup> L. Velázquez<sup>d</sup> and E. F. da Silveira<sup>\*a</sup>

<sup>a</sup> Departamento de Física, Pontifícia Universidade Católica do Rio de Janeiro, Rua Marquês de São Vicente, 225, CP 38071, 22452-970 Rio de Janeiro, Brazil. E-mail: enio@fis.puc-rio.br (E. F. da Silveira); Fax: 55 2131141040; Tel: 55 2131141272

<sup>b</sup> Instituto Superior de Tecnologías y Ciencias Aplicadas, Ave Salvador Allende esq Luaces, s/n CP 10600, AP.6163 Ciudad de la Habana, Cuba

<sup>c</sup> Instituto de Química, Universidade Federal do Rio de Janeiro, Cidade Universitaria, CT Bloco A sala 412, Rio de Janeiro, RJ 21949-900, Brazil

<sup>d</sup> Departamento de Física, Universidad de Pinar del Río, Martí 270, Esq. 27 de Noviembre, Pinar del Río, CP: 20100, Cuba

Received 22nd November 2004, Accepted 9th March 2005

First published as an Advance Article on the web 21st March 2005

(CsI)<sub>n</sub>Cs<sup>+</sup> ( $n = 1, 2$ ) cluster ion formation from polycrystalline CsI irradiated by pulsed-UV laser (337 nm) is analyzed by delayed extraction time-of-flight mass spectrometry technique. Measurements were performed for different laser intensities and for several delayed extraction times. Experimental data show that CsI laser ablation produces the emission of (CsI)<sub>n</sub>Cs<sup>+</sup> ions ( $n = 0, 1, 2$ ), whose yields decrease exponentially with  $n$  and increase exponentially with the laser pulse energy. A quasi equilibrium evolution of the clusters is proposed to extract a parameter characteristic of the cluster recombination process. The delayed extraction method of initial velocity determination was improved to take into account collisions in the high density plasma close to the target. The new parameterization helps to describe the dynamics of secondary ions of different masses for laser irradiances above the ion desorption threshold in a collision regime. The initial velocity of the secondary ions [(CsI)<sub>n</sub>Cs<sup>+</sup> ( $n = 0, 1, 2$ )] as function of the laser irradiance was determined. The distance to the target when the free expansion process starts is reported as function of the secondary ions mass and of the laser irradiance. The collision regime's influence on the secondary ion dynamics is discussed.

## Introduction

Lasers have been used in the last three decades to produce high-temperature and high-density plasmas for fusion devices by vaporizing a small amount of material with high-powered nanosecond pulses. The process is called laser ablation, and is now widely used for both the deposition and patterning of thin films. To achieve a useful high deposition rate, the laser irradiance is chosen for heating the solid above its normal boiling point. The vapor evolved from the laser heated surface strongly absorbs the laser, though the absorption processes have not yet been clarified.

Several approaches have been used to describe the laser ablation process: analytical models based on self-regulating absorption *via* inverse bremsstrahlung (IB)<sup>1</sup> are successful when the laser irradiance is high enough to fully ionize the plasma in the early stage of the pulse; models considering that the vapor absorption reduces the amount of material removed<sup>2</sup> (without heating or producing ionization in the vapor); models assuming that photo-absorption (photo-ionization of the excited states) and collisional processes produce plasma;<sup>3</sup> models including the shielding of the target by IB;<sup>4</sup> and numerical models based on solid heating and evaporation by laser, as well as vapor heating, ionization and expansion.<sup>5</sup>

The experimental study of such a phenomenon demands techniques capable of probing the plasma plume at different

moments of its evolution. In particular, the delayed extraction (DE) technique's capability of dealing with the initial energy distribution of emitted ions allows the possibility of probing different stages of the evolution of the laser created plasma.

Delayed extraction has been widely used in high performance laser desorption time-of-flight (TOF) mass spectrometry (MS) since the middle of the nineties. The technique was originally introduced in 1955 by Wiley and McLaren, as "time-lag energy focusing",<sup>6</sup> to improve the mass resolution of TOF spectrometers with electron impact ionization of gas targets. In DE, the correct choice of both the delay time and the value of the extraction potential, allows the initially slow ions—which spend a longer time under the extraction field's action—to receive enough additional kinetic energy to catch the initially fast ions of the same mass-charge ratio right at the detector surface.

In 1983, Tabet and Cotter<sup>7</sup> pointed out the convenience of using DE technique as a method for measuring ion initial energies. In 1990 Spengler and Cotter<sup>8</sup> used the method to obtain mass spectra of heavy biomolecules in an instrument with orthogonal configuration, also determining the initial kinetic energy distribution of the emitted ions. Determination of the initial velocity of the emitted ions using DE was studied theoretically and experimentally by Juhasz *et al.*<sup>9</sup> In their work, they have shown that the ion TOF changes linearly with the extraction delay, making it possible to determine the initial velocity of the ion from the slope of this dependence. For this, they assumed that the ion's initial velocity does not depend on the laser pulse duration, the laser pulse's intensity or the

† Presented at the Third International Meeting on Photodynamics, Havana, Cuba, February 16–20, 2004.

post-generated ion evolution collisions effect. The DE technique has been applied also to the study of the ablation of inorganic samples.<sup>10,11</sup>

Cesium iodide has a simple chemical composition, both atomic species are mono-isotopic, which simplifies mass-spectrometric analyses, and is convenient for the study of the physical aspects of the ablation process. On the other hand, CsI highly absorbs UV light, producing a large number of Cs ions and an abundant  $(\text{CsI})_n\text{Cs}^+$  cluster population ( $n = 1$  and  $2$ ). All these characteristics make CsI interesting as a model target for laser induced cluster formation studies.

We have previously reported a thermal ablation model to describe the ion dynamics of the Cs ions created by UV laser in the first stages of its temporal evolution (0 to 150 ns).<sup>12</sup> The model was used to describe the plume temperature evolution during its expansion using DE-TOF-MS spectra at different laser irradiances. As a series of ion clusters is observed experimentally and the cluster emission cannot be predicted by standard evaporation models, the investigation of the ablation process remains an open subject.

In this article, the experimental results and ion dynamics simulations of laser sputtering of cesium iodide clusters are presented. A linear TOF mass spectrometer, equipped with DE field ion source, was used for the analysis of  $(\text{CsI})_n\text{Cs}^+$  ( $n = 0, 1, 2$ ) ion sputtering. The ion cluster yield, as a function of the applied laser irradiance, and the effective temperature characteristic of the cluster recombination are also reported. The cluster's initial velocities are determined from dynamics simulations of the DE TOF spectra; the leakage field effects are described based on a previous reported study of ion dynamics and peak shapes.<sup>13</sup> The DE-TOF method is used to measure the distance of the ions from the target and the ions' velocity when the free expansion starts.

## Experimental

All experiments were carried out in a homemade two-stage ion source linear TOF mass spectrometer equipped with a DE system. The 337 nm radiation from a nitrogen laser (VSL-337-ND-S, Laser Science Inc.) was brought into focus on the target with a 30° incidence angle after passing through a gradient neutral density Oriol attenuator (as shown in Fig. 1).

The ion extraction region is composed of two stages, each one ended by a 90% transmission electroformed nickel grid (Buckbee Mears) of 70 wires per inch. The target was mounted on a precision X-Y-Z manipulator. The distance from the target to the first grid ( $d_1$ ) was varied looking for the best conditions to observe the effects of the DE technique on the spectra. The distance between the first and second grids ( $d_2$ )

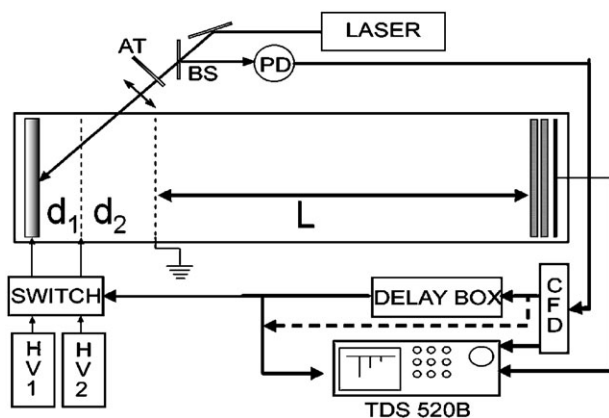


**Fig. 1** Schematic diagram of the mass spectrometer. AT – gradient neutral density attenuator, BS – beam splitter, PD – photodiode, HV1 and HV2 – high voltage power supplies, TDS-520B – digital oscilloscope, CFD – constant fraction discriminator. The thick dashed line shows a second option for start signal generation also used.

was fixed at  $20.0 \pm 0.1$  mm (or  $17.7 \pm 0.1$  mm when specified). The drift tube length  $L$  is  $276.5 \pm 0.1$  mm (or  $1376.0 \pm 0.1$  mm when specified). Two high stability power supplies (HCN 14-20000 and HCN 35-30000, F.u.G. Elektronik GmbH) were used to bias the target holder and the first grid. A pair of microchannel plates mounted in chevron configuration was used as ion detector.

The DE system is based on a high voltage fast switch HTS 300 (Behlke Electronics). The switch triggers a high-voltage positive pulse which changes the target electrode potential from  $U_0$  to a higher value  $U_1$ . A voltage rise-time of *ca.* 110 ns was observed, and the delay time between laser and extraction pulses was varied from 200 ns up to 1200 ns using three delay boxes (DB463, EG&G ORTEC).

CsI (99.9% purity, Merck) polycrystalline films, grown over stainless steel substrates by deposition in an evaporation chamber at a pressure of  $10^{-5}$  mbar, were used as targets.

## Results and discussion

### Prompt extraction

In Fig. 2, the  $(\text{CsI})_n\text{Cs}^+$  TOF spectrum corresponding to  $I = 1.69 \text{ GW cm}^{-2}$  shows that the relative abundance of the different clusters decreases exponentially.

To determine the cluster emission yield characteristics, the laser irradiance was varied. As shown in Fig. 3, the yield increases because both the peak amplitude and peak width increase as the laser irradiance increases.

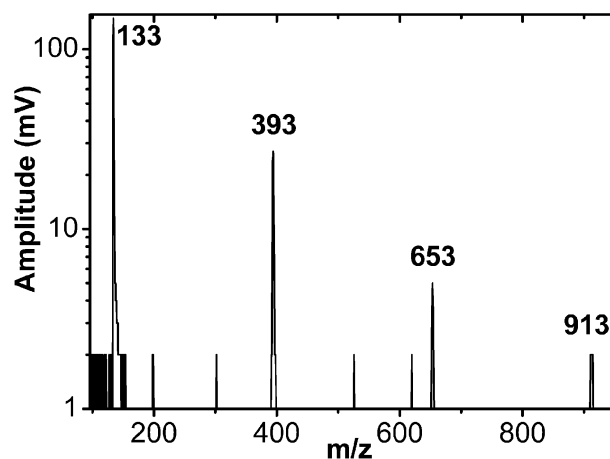
Actually, as illustrated for  $n = 1$  in Fig. 4, the desorbed ion yield grows slightly faster than their mean energy as a function of the laser irradiance increment, for all the observed clusters. The left side of the TOF peak reveals the formation of the more energetic ions and the right part reveals an increment in the formed plasma density. The increase in the plasma density forces the desorbed particles (ions and neutrals) mean free path to decrease in the primary stages of the plasma expansion, delaying the beginning of the free collision expansion process for the slower particles.

Fig. 3 shows that the cluster ion production increases exponentially with the laser irradiance ( $I$ ) and decreases, also exponentially, with the number  $n$  of CsI units:

$$Y \propto e^{pI - qn} = e^{pI} e^{-qn} \quad (1)$$

The values of the parameters are  $p \sim 5 \text{ GW}^{-1} \text{ cm}^2$  and  $q \sim 1.6$ .

A possible interpretation of the above exponential behaviour of species' abundance on their mass, observed experimentally, could be as follows. The laser ablation produces a high density ionized gas formed by atomic species. It has been claimed that



**Fig. 2**  $(\text{CsI})_n\text{Cs}^+$  ( $n = 0..3$ ) ions clusters TOF spectrum induced by laser desorption. The spectrometer parameters are:  $U_1 = 9.7 \text{ kV}$ ,  $U_0 = 9.0 \text{ kV}$ ,  $d_1 = 0.45 \text{ cm}$  and laser irradiance  $I = 1.69 \text{ GW cm}^{-2}$ .

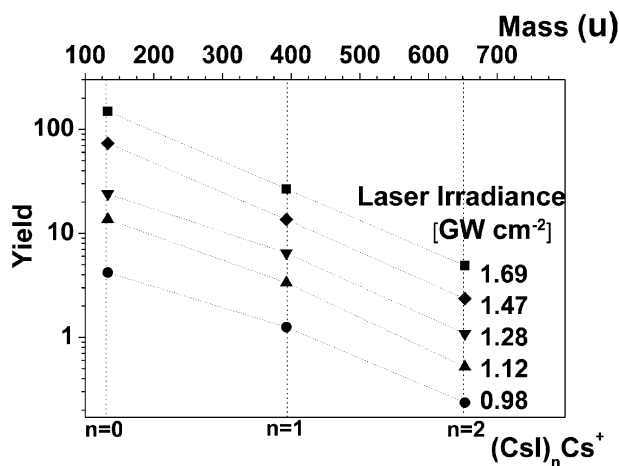


Fig. 3  $(\text{CsI})_n\text{Cs}^+$  ( $n = 0, 1, 2$ ) ion cluster yields as function of the cluster mass, for different laser irradiances. The spectrometer parameters are:  $U_1 = 9.7$  kV,  $U_0 = 9.0$  kV and  $d_1 = 0.45$  cm.

in laser induced desorption, the very fast warming up ( $10^{10}$  K  $\text{s}^{-1}$ ) favours emission of aggregates.<sup>14</sup> However, considering the high temperature observed in the plasma produced by laser ablation,<sup>12,15,16</sup> a more reasonable assumption is that in the primary stages the plasma is mainly composed of atomic species. The gas temperature drops during its expansion, which leads to a recombination of the atomic species, *i.e.* the formation of the clusters. Since the energy of the cluster varies almost linearly with its mass (see Fig. 5), eqn. (1) can be rewritten in terms of the clusters' energies, in this case assuming a form of a canonical distribution, which suggest the existence of a quasi-equilibrium evolution of the gas as:

$$N_n(I) = C(I)e^{-\beta^*(I)\varepsilon_n} \quad (2)$$

where  $N_n$  and  $\varepsilon_n$  represent the  $n$ th species abundance and its energy, respectively,  $I$  is the laser irradiance,  $C(I)$  is a factor proportional to  $\exp(pI)$ , and  $\beta^*(I) \propto 1/T^*(I)$  is a quantity that could be related to an effective temperature,  $T^*$ , characteristic of the recombination process in such conditions. The assumption of quasi equilibrium evolution of the gas has been used by other authors.<sup>17–21</sup>

Apparently, this quasi-equilibrium evolution arises due to a characteristic recombination rate larger than the gas expansion rate. Notice that the effective temperature is negative (different from the gas temperature), which is characteristic for systems with an inverse particle population. The species' abundance depends on the laser's irradiance and varies during the gas

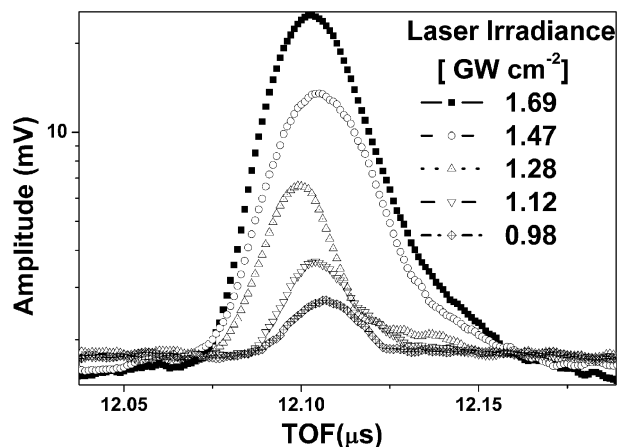


Fig. 4  $(\text{CsI})_n\text{Cs}^+$  ion cluster TOF spectrum obtained by laser desorption. The spectrometer parameters are:  $U_1 = 9.7$  kV,  $U_0 = 9.0$  kV,  $d_1 = 0.45$  cm and laser irradiance was varied from  $I = 0.98$  to  $1.69$   $\text{GW cm}^{-2}$ .

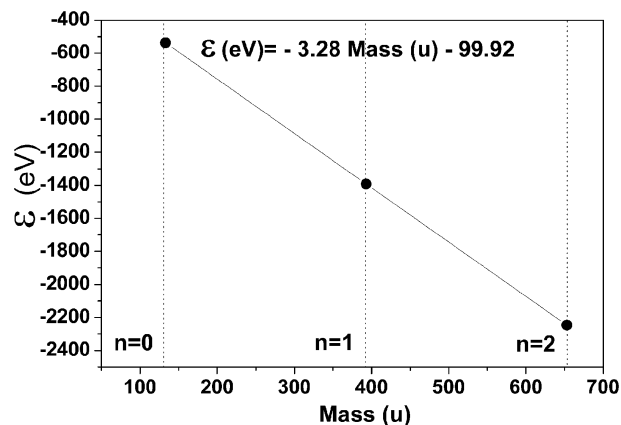


Fig. 5  $(\text{CsI})_n\text{Cs}^+$  ion energy ( $\varepsilon$ ) dependence on its mass. The energy values were calculated at the DFT B3LYP/LACV3P level, using the Jaguar 5.5 software.<sup>22</sup>

expansion, up to the point where the free expansion is achieved (non-interactive system) and the recombination is not possible any longer. The effective temperature observed experimentally corresponds to the time when the free expansion regime is reached. From Fig. 3 it can be seen that the relative species' abundances do not depend on the laser's irradiance; consequently, neither does the effective temperature. Eqn. (2) could be rewritten as:

$$N_n(I) = C(I)e^{-\beta^*\varepsilon_n} \quad (3)$$

To determine the  $\beta^*$  value, characteristic of the recombination process, the energy of the clusters were optimized at the DFT B3LYP/LACV3P level, using the Jaguar 5.5 software<sup>22</sup> and all the vibrational frequencies were verified to be real. The use of DFT energies follows from the fact that, according to eqn. (1), the yield depends on  $\exp(-qn)$ , where  $n$  is proportional to the cluster mass. Furthermore, from Fig. 5, the mass of the cluster, in its turn, is proportional to its DFT energy. Thus,  $(-qn) \sim (-qm_n) \sim (-\beta\varepsilon_n)$ , as in eqn. (2). The DFT calculation furnished the energy values of  $\varepsilon_0 = -537.05$  eV,  $\varepsilon_1 = -1392.03$  eV and  $\varepsilon_2 = -2246.46$  eV, respectively, for  $(\text{CsI})_n\text{Cs}^+$  ( $n = 0, 1, 2$ ). Once the clusters' energies are known, the value of  $\beta^*$  can be determined from the ratio of the species' abundance, for any two members of the clusters series.

From the values presented in Fig. 3, one obtains  $1/\beta^*$  equal to  $-502.5 \pm 12.6$  eV. As the measured  $N_n(I)/N_{n+1}(I)$  does not depend on laser irradiance, neither does the value of  $\beta^*$ . The parameter  $\beta^*$  characterizes the recombination process of cesium iodide ion clusters during the gas expansion of a UV 337 nm laser created plasma.

#### Delayed extraction

The theoretical grounds for the secondary ions initial velocity determination in a "no-collision" regime by DE-TOF-MS are reviewed in the Appendix, together with a short discussion supporting the extension for a collision regime.

Fig. 6 presents the measured TOF spectra for increasing extraction delay times,  $\tau$ . Two main observations follow from the data. The first, an obvious consequence of delaying the extraction field, is the progressive late arrival of the SI at the stop detector. Each TOF peak is shifted by an amount which is approximately equal to  $\tau$ . The  $\text{Cs}^+$  TOF signal shows no variation for values of  $\tau$  larger than 900 ns, implying that the fastest ions need this time interval to cross the first acceleration region distance with an approximate velocity of  $3.4$   $\text{km s}^{-1}$ . If the leakage field is taken into account (a leakage field of  $\varepsilon_0 = 56$   $\text{V cm}^{-1}$  in our case), an approximate velocity for the fastest ions of  $2.0$   $\text{km s}^{-1}$  is obtained. This result overestimates the initial ion velocity but agrees better with the previously

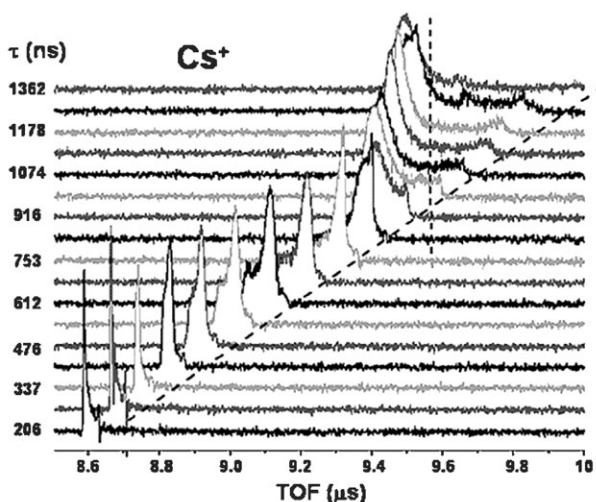


**Fig. 6**  $\text{Cs}^+$  ion TOF spectra as a function of the extraction delay time ( $\tau$ ). The experimental parameters are:  $U_1 = 6.7$  kV,  $U_0 = 6.0$  kV,  $d_1 = 0.35$  cm and laser irradiance  $I = 0.74$  GW  $\text{cm}^{-2}$ . Note the peak tail flipping at  $\tau \sim 270$  ns and the constant TOF for the fastest ions at  $\tau > 900$  ns.

reported initial ion velocity (*ca.*  $1.3$  km  $\text{s}^{-1}$  for the mean velocity when the plasma formation was considered<sup>12</sup>).

The second observation is better seen when the TOF- $\tau$  is plotted as a function of  $\tau$ . The delay TOF- $\tau$  is linear to the SI initial velocity, since the faster it is, the smaller is the acceleration region available for the ion when the extraction field is applied and, therefore, the smaller is its final velocity.<sup>9</sup> As a consequence, the TOF peak width decreases as  $\tau$  increases, until the best time resolution  $\tau_c$  (named the critical delay) is reached after which it begins to spread out, reversing its peak shape (Fig. 6). The evolution of the peak shape as a function of the delay time shows that its flipping occurs at around 270 ns, as previously described by the ions dynamic simulation in a DE TOF experiments.<sup>12,13</sup>

In the absence of collisions in the plume, the initial axial velocity of the desorbed ions would be the same whatever the extraction delay range used to measure it. In the desorption process, the ions are essentially emitted in a direction perpendicular to the target surface but, due to collisions in the plume, the radial velocity increases while the axial velocity decreases, until both radial and axial remain constant when a free collision expansion state is reached. This behaviour has been observed in plasma plumes using other techniques.<sup>16,23,24</sup>

The two major difficulties of this method are: (a) the determination of the leakage field effects in the first acceleration region and (b) the definition of the distance from the target at which the free expansion of the plume starts.

The first difficulty is related to the fact that, in spite of the first grid potential being the same as that of the target during the delay time,  $\tau$ , the permanent and high electric field (*ca.*  $300$  v  $\text{mm}^{-1}$ ) of the second acceleration region leaks into the first one (see Fig. 1). This leakage field is intense enough to increase substantially the low kinetic energy (few eV) of the emitted ions. The experimental data presented in this work have been analyzed by a procedure described in ref. 13, based on SIMION 6.0 simulations of the electric field generated by the grids.

The second difficulty touches basic concepts: in a "collision" regime, the very initial velocity (at the target surface) is different from the "initial" velocity when the free expansion starts. How can one determine the "initial" energy without having a model for the plume expansion? Is it possible to define an average distance from the target (dependent on the laser's irradiance,  $d_0(I)$ , beyond which no further collision occurs inside the plume? The main concern is whether the DE-TOF method is capable of measuring both: this distance and the ion's velocity when its free expansion starts.

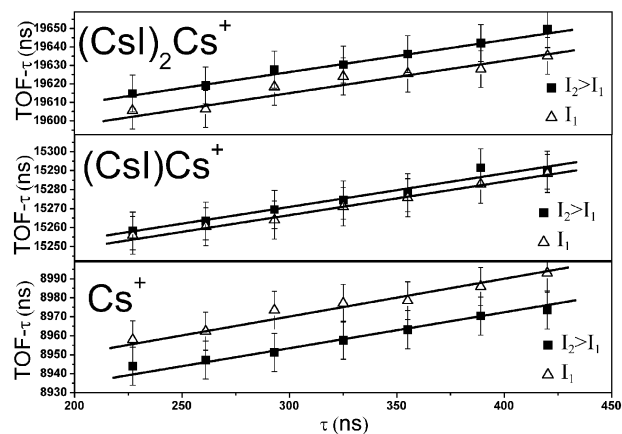


**Fig. 7** The value of TOF- $\tau$  as a function of the extraction field delay  $\tau$  for  $(\text{CsI})_n\text{Cs}^+$  ( $n = 0, 1, 2$ ) ions. The spectrometer parameters are:  $U_1 = 18.0$  kV,  $U_0 = 14.0$  kV,  $d_1 = 0.61$  cm,  $d_2 = 1.77$  cm and  $L = 137.6$  cm. The laser irradiances are  $I_1 = 0.92$  GW  $\text{cm}^{-2}$  and  $I_2 = 2.16$  GW  $\text{cm}^{-2}$ .

If, on one hand, more laser power means more energy incorporated into the system (more secondary ion (SI) kinetic energy and shorter TOF), on the other hand it also means higher density plasma, more SI collisions, shielding from the laser radiation and from the external extraction electric field (which implies a longer TOF).

For the configuration described in Fig. 6, a low laser irradiance  $I = 0.74$  GW  $\text{cm}^{-2}$  was chosen to avoid these last effects. Under these conditions the free expansion of the SI's practically originates at the target surface and its evolution is predicted by the standard "no-collision" formalism of the delayed extraction.<sup>9,13</sup> In contrast, Fig. 7 presents data obtained at two higher laser irradiances,  $I_1 = 0.92$  GW  $\text{cm}^{-2}$  and  $I_2 = 2.16$  GW  $\text{cm}^{-2}$ , for the  $(\text{CsI})_n\text{Cs}^+$  ( $n = 0, 1, 2$ ) ions, respectively.

In the "no-collision" regime more laser irradiance means more SI kinetic energy (steepest slope) and shorter TOF; however, these predictions are not in agreement with data presented in Fig. 7 for the two laser irradiances, both higher than the one used to obtain the data in Fig. 6. Note that for each delay time,  $\tau$ , and each laser irradiance,  $I$ , the TOF's values were obtained from the same spectrum. Therefore the time interval between the TOF's of the different clusters is indeed reliable. The delay times used are longer than the corresponding critical delays  $\tau_c$ , which in turn are shorter than 10 ns for all the ions presented in Fig. 7. The TOF- $\tau$  vs.  $\tau$  plots of Fig. 7 show two main features: (i) the slopes are the same for the two laser irradiances; (ii) the TOF shift varies with the cluster mass. Both features are evidence of plasma formation in a "collision" regime.

### The "collision" regime

To fit the data consistently with the laser irradiance's dependence, we have introduced a new parameter for taking into account the collisions in the plasma near the surface. It is assumed that over a distance  $d_0(I)$  to the target (*i.e.* plasma thickness), the SI's are shielded from the externally applied extraction field (including the leakage field). The data presented in Fig. 7 were fitted with two free parameters, the "initial" velocity,  $v_0(I)$ , and the distance of the SI to the target,  $d_0(I)$ , when the free expansion starts. The simulations were performed taking into account the leakage field influences, after the free expansion, and the ion dynamics inside the spectrometer. The values are displayed in Table 1.

The following scenario is proposed to describe the processes giving rise to the measured data, summarized in Table 1. During the laser shot (few ns), the heated solid surface sublimates into a very hot plasma formed by electrons and by

**Table 1** Simulation results for the “initial” velocity ( $v_0(I)$ ) and the distance from the target ( $d_0(I)$ ), when the free expansion starts, as function of the laser irradiance for the  $(\text{CsI})_n\text{Cs}^+$  ( $n = 0, 1, 2$ )  $\text{SI}^a$

SI	$m/u$	$v_0/m \text{ s}^{-1}$		$d_0/\mu\text{m}$	
		$I_1$	$I_2 > I_1$	$I_1$	$I_2 > I_1$
$\text{Cs}^+$	133	1117 ± 270	1052 ± 260	635 ± 42	520 ± 40
$(\text{CsI})_1\text{Cs}^+$	393	646 ± 175	661 ± 180	198 ± 12	206 ± 10
$(\text{CsI})_2\text{Cs}^+$	653	455 ± 150	516 ± 140	68 ± 11	82 ± 14

<sup>a</sup> Laser irradiances correspond to  $I_1 = 0.92$  and  $I_2 = 2.16 \text{ GW cm}^{-2}$ .

atomic species (neutral and ions). Models predict temperatures up to  $10^5 \text{ K}$ .<sup>12,16</sup> The ejected material moves away from the target surface in a planar and spreading shock wave, very dense, which can be divided into three main regions:<sup>25,26</sup> (a) the frontal or external region, formed by the fastest particles; (b) the central region, characterized by the highest pressure in the plasma, capable of producing clusters; (c) the internal or confined region, close to the surface, having lower density, temperature and cluster abundance relative to the central region. In this picture,  $\text{Cs}^+$  ions exist all over the plasma cloud; however, the heavier the cluster the narrower is its distribution in the central region.

The particles of the external region (fastest ions) generate the left side of the TOF peak (see Fig. 4): they expand almost freely and, when the laser’s irradiance increases, they become faster (shorter TOF) and their number also increases. However, this behaviour is not homogeneous and the central region suffers more collisions with the gas core (heavy clusters) during its expansion when the laser irradiance increases. Such collision effect can be observed from the comparison of the “initial” velocities when the free expansion starts, as shown in Table 1.

The heavy clusters (essentially  $n = 2$  member, in the present case) are formed in the central part of the cloud and are very sensitive to the laser’s irradiance. They typically take 150 ns to reach the collision-free expansion regime, after which they cannot be formed any more. Their  $v_0$  and  $d_0$  values increase as laser irradiance increases.

The light ions ( $n = 0$  and 1) present in the confined region suffer the highest number of collisions, approaching the thermodynamical equilibrium, which explains their velocities being higher than those of  $n = 2$ . As they are kept together for a longer time (300–600 ns), the distance they need to travel up to their free expansion is also longer ( $d_0 \sim 200$ –600  $\mu\text{m}$ ). The high abundance of the  $\text{Cs}^+$  ions in the confined region may also explain the peculiar behaviour of these ions, which have decreasing average values of  $v_0$  and  $d_0$  when the laser irradiance increases. Note finally that the  $n = 1$  cluster exhibits an intermediate behaviour between those of the  $n = 0$  and  $n = 2$  species.

## Conclusions

The laser induced formation of CsI ion cluster was studied for UV 337 nm laser irradiances in the range of 0.7–2.1  $\text{GW cm}^{-2}$  by delayed extraction time of flight mass spectrometry. It is shown that the  $(\text{CsI})_n\text{Cs}^+$  ( $n = 0, 1, 2$ ) secondary ion yields can be described by the product of two terms: the first one represents the mechanism of energy absorption/deposition ( $\exp(p^*I)$ ) and the second one is proportional to the probability of the atomic species’ recombination during the expansion of a highly density ionized cloud ( $\exp(-q^*n)$ ). The assumption of a quasi-equilibrium evolution of the clusters supports the description of the recombination process by a characteristic parameter independent of the laser’s irradiance.

The “non-collision” and the “collision” regimes for low and high laser irradiances, respectively, were discussed. The new proposed parameterization of the delayed extraction method

helps the description of the secondary ions dynamics in a “collision” regime. The distance of the plume to the target, when the free expansion starts, and the ion velocity beyond this point can be determined by this method and are reported for the CsI analyzed ion series. The influence of the “collision” regime on the secondary ion dynamics is such that the heavier particles receive more kinetic energy than the light ones when the laser irradiance increases.

## Appendix

In a linear two-stage acceleration TOF system, the initial ion velocity ( $v_0$ ) can be determined as an approximation of the slope of the flight time curve vs. extraction delay. For this purpose, flight times and their dependence on the delay time are measured and an analytical solution/approximation of the flight time equation is used to determine  $v_0$  (DE-Vestal method<sup>9,27,28</sup>).

Briefly, the time-of-flight (TOF) equations can be written as function of the two grid distances ( $d_1$  and  $d_2$ ), the field free drift length ( $L$ ), the delay time ( $\tau$ ), the sample target potentials ( $U_0$  and  $U_1$ : initially  $U_0$  switches into  $U_1$  after the delay time  $\tau$ ), the first grade potential ( $U_0$ ), the mass ( $m$ ) and the charge ( $q$ ) as follows:

$$\text{TOF}(\tau, v_0) = \text{TOF}(0,0) + \tau + \left( \eta\tau - \frac{2d_1}{v_R} \right) \left( \frac{v_0}{v_R} \right) + \left( \tau - \frac{\eta d_1}{v_R} \right) \left( \frac{v_0}{v_R} \right)^2 \quad (\text{A1})$$

where:

$$\eta = R\sqrt{R} \frac{L}{2d_1} + \frac{R}{1 + \sqrt{R}} \frac{d_2}{d_1} - 1, \quad v_R = \sqrt{\frac{2q}{m}(U_1 - U_0)}, R = \frac{U_1 - U_0}{U_1} \quad (\text{A2})$$

$\text{TOF}(0,0)$  is the time of flight for an ion “emitted” with  $v_0 = 0$  and extracted promptly ( $\tau = 0$ ):

$$\text{TOF}(0,0) = \frac{d_1}{v_R/2} + \frac{d_2}{v_R/2} \left( \frac{\sqrt{R}}{1 + \sqrt{R}} \right) + \frac{L}{v_R} \sqrt{R} \quad (\text{A3})$$

which represents the sum of time intervals that the ion takes to travel the distances  $d_1$ ,  $d_2$  and  $L$ , respectively.

Assuming  $\tau \ll d_1/v_0$ ,  $v_0 \ll v_R$  and considering the plot  $\text{TOF}(\tau, v_0) - \tau$  vs.  $\tau$ , the slope of the function can be written as:

$$\frac{d(\text{TOF} - \tau)}{d\tau} = \eta \frac{v_0}{v_R} = \frac{v_0}{v_{\text{ref}}} \quad (\text{A4})$$

where:

$$v_{\text{ref}} = \frac{v_R}{\eta} = \frac{1}{R^{3/2} \frac{L}{2d_1} + \frac{R}{1 + \sqrt{R}} \frac{d_2}{d_1} - 1} \sqrt{\frac{2q}{m}(U_1 - U_0)} \quad (\text{A5})$$

One can see from eqn. (A4), that the initial velocity  $v_0$  of the desorbed ions can be determined from the measurements of the slope  $d(\text{TOF} - \tau)/d\tau$ . In fact, the distributions of the slope of each part of the TOF peak allow, in principle, the determination of the initial velocity distribution.

In a higher order approximation, the shape of the velocity distribution should also be taken into account. At short extraction delays, the ions may have not reached their “final” initial velocity and collisions with neutrals can slow ions down. The time lag, until a free expansion regime can be considered, has been estimated from hydrodynamic calculations to be about 50–100 ns.<sup>29</sup> Therefore, the time lag also depends on the laser’s irradiance due to the substantial interaction between ions and neutrals.

To estimate the volume occupied by this initially expanding and interacting system as function on the laser's irradiance, a new parameter,  $d_0$  can be introduced into eqn. (1): the length  $d_0$  corresponds to the distance travelled by the desorbed ions until their velocity becomes constant ("final" initial velocity). Once the free expansion regime is reached, their "final" initial velocity is considered as the new "initial" velocity for the movement described by eqn. (1).

## Acknowledgements

The authors acknowledge the Centro Latinoamericano de Física, FAPERJ and CNPq for the partial support of this work.

## References

- 1 F. Piuze, *Nucl. Instrum. Methods, Phys. Res., Sect. A*, 1996, **371**, 96–115.
- 2 S. Fähler and H. U. Krebs, *Appl. Surf. Sci.*, 1996, **96–98**, 61.
- 3 D. I. Rosen, J. Mitteldorf and G. Pugh, *J. Appl. Phys.*, 1982, **53**, 3190.
- 4 J. Almeida, A. Amadon, P. Besson, P. Bourgeois, A. Braem, A. Breskin, A. Buzulutskov, R. Chechik, C. Coluzza, A. Di Mauro, J. Friese, J. Homolka, F. Iacovella, A. Ljubici, Jr., G. Margaritondo, Ph. Miné, E. Nappi, T. dell'Orto, G. Paic, F. Piuze, F. Posa, J. C. Santiard, P. Sartori, S. Sgobba, G. Vasileiadis and T. D. Williams, *Nucl. Instrum. Methods Phys. Res., Sect. A*, 1995, **367**, 332–336.
- 5 A. Breskin, *Nucl. Instrum. Methods Phys. Res., Sect. A*, 1996, **371**, 116–136.
- 6 W. C. Wiley and I. H. McLaren, *Rev. Sci. Instrum.*, 1955, **26**, 1150.
- 7 J. C. Tabet and R. C. Cotter, *Int. J. Mass Spectrom. Ion Processes*, 1983, **54**, 151.
- 8 B. Spengler and R. J. Cotter, *Anal. Chem.*, 1990, **62**, 793.
- 9 P. Juhasz, M. L. Vestal and S. A. Martin, *J. Am. Soc. Mass Spectrom.*, 1997, **8**, 209.
- 10 Y. Choi, H. Im and K. Jung, *Int. J. Mass Spectrom.*, 1999, **189**, 115.
- 11 Y. Choi, H. Im and K. Jung, *Appl. Surf. Sci.*, 1999, **150**, 152.
- 12 F. Fernandez-Lima, V. M. Collado, C. R. Ponciano, L. S. Farenzena, E. Pedrero and E. F. da Silveira, *Appl. Surf. Sci.*, 2003, **217**, 202.
- 13 V. M. Collado, C. R. Ponciano, F. A. Fernandez-Lima and E. F. da Silveira, *Rev. Sci. Instrum.*, 2004, **75**, 2163.
- 14 L. Hanley, O. Kornienko, E. T. Ada, E. Fuoco and J. L. Trevor, *J. Mass Spectrom.*, 1999, **34**, 708.
- 15 J. G. Lunney and R. Jordan, *Appl. Surf. Sci.*, 1998, **127–129**, 941–946.
- 16 J. G. Lunney and R. Jordan, *Appl. Surf. Sci.*, 1998, **127–129**, 968–972.
- 17 R. Kelly and R. W. Dreyfus, *Nucl. Instrum. Methods Phys. Res., Sect. B*, 1988, **32**, 341.
- 18 R. Kelly and R. W. Dreyfus, *Surf. Sci.*, 1988, **198**, 263.
- 19 L. V. Zhigelei and B. J. Garrison, *Appl. Phys. Lett.*, 1997, **71**, 551.
- 20 W. Zhang and B. T. Chait, *Int. J. Mass Spectrom. Ion Processes*, 1997, **160**, 259–267.
- 21 A. A. Puzosky, D. B. Geoghegan, G. B. Hurst and M. V. Buchanan, *Phys. Rev. Lett.*, 1999, **83**, 444–447.
- 22 Jaguar 5.5, Schroedinger Inc. Portland, Oregon, 2004.
- 23 E. Moskovets and A. Vertes, *J. Phys. Chem. B*, 2002, **106**, 3301–3306.
- 24 A. Mele, A. Giardini Guidoni, R. Kelly, A. Miotello, S. Orlando and R. Teghil, *Appl. Surf. Sci.*, 1996, **96–98**, 102.
- 25 R. K. Singh and J. Narayan, *Phys. Rev. B*, 1990, **41**, 8843.
- 26 R. Kelly and A. Miotello, *Nucl. Instrum. Methods Phys. Res., Sect. B*, 1997, **122**, 374.
- 27 P. Juhasz, M. T. Roskey, I. P. Smirnov, L. A. Haff, M. L. Vestal and S. A. Martin, *Anal. Chem.*, 1996, **68**, 941.
- 28 M. L. Vestal, P. Juhasz and S. A. Martin, *Rapid Commun. Mass Spectrom.*, 1995, **9**, 1044.
- 29 A. Vertes, G. Irinyi and R. Gijbels, *Anal. Chem.*, 1993, **65**, 2389.